Kinetics and Mechanism of the Heterogeneous Oxidation of Methyl Radicals on Samarium(III) Oxide. Implications for the Oxidative Coupling of Methane

V. T. Amorebieta and A. J. Colussi*

Contribution from the Department of Chemistry, University of Mar del Plata, 7600-Mar del Plata, Argentina

Received October 25, 1994[⊗]

Abstract: The purely heterogeneous oxidation of $CH_3(g)$ on Sm_2O_3, in the presence and absence of $O_2(g)$, was investigated in a very low pressure flow reactor by molecular beam mass spectrometry, between 1000 and 1200 K. In the presence of O_2, CH_3 is quantitatively oxidized to H_2O and CO_x at steady state rates proportional to $[CH_3]\Gamma_5([O_2]) = [CH_3]k_5K_5^{1/2}[O_2]^{1/2}/(1 + K_5^{1/2}[O_2]^{1/2})$. Alternate or simultaneous measurement of oxidation rates for CH_3 and CH_4, the latter proportional to $[CH_4]\Gamma_4([O_2])$, on the same Sm_2O_3 sample as a function of $[O_2]$ and temperature, led to the following expressions: $\log(k_5/k_4) = -(2.18 \pm 0.35) + (3210 \pm 301)/T$ (1), $\log(K_4/10^9\ \mathrm{M}) = (1.89 \pm 0.25) - (4170 \pm 260)/T$ (2), $\log(K_5/10^9\ \mathrm{M}) = (5.65 \pm 0.11) - (6480 \pm 130)/T$ (3). Equations 1−3 imply that (1) *methyl radicals are oxidized faster than methane on Sm_2O_3 below 1500 K* and (2) *each reaction occurs on distinguishable active sites generated by endothermic, but highly exentropic, O_2 chemisorptive processes involving cooperative participation of the solid.* Transient experiments provide evidence on the relative timing of O_2 chemisorption, CH_3 oxidation, and CO_2 release. Sm_2O_3 is almost inert under anoxic conditions. Present results impose an irreducible floor to CO_x yields in the *steady state* oxidation of methane on Sm_2O_3 at low pressures, but open up the possibility of disengaging CH_3 and CH_4 oxidations under other conditions.

Introduction

It is widely agreed that the partial oxidation of methane on various metal oxides begins with the generation of methyl radicals:

$$CH_4(g) + \alpha_xO(s) \rightarrow \beta CH_3(g) + (1 - \beta)CO_x + \{2 - (3\beta/2)\}H_2O \quad (4)$$

followed by CH_3 dimerization or further oxidation.[1-6] If the goal is to maximize the yield of C_2 species, the production of the thermodynamically favored waste carbon oxides must be kinetically controlled.[7,8] In this context, it seems essential to fully understand the mechanism of oxidation of methyl radicals in these systems.[4,9-11]

Methyl radicals can be oxidized *in ovo*, i.e. while being formed ($\beta < 1$). Of those which desorb, some may undergo combustion in the gas phase, and the rest return to the surface for secondary oxidation. We have recently studied the $CH_3(g) + O_2(g)$ reaction at high temperatures.[12,13] We now conduct experiments specifically designed to investigate the latter possibility.

It should be emphasized that the heterogeneous process of interest can only be isolated by working at sufficiently low pressures.[6] This proviso, not always realized or implemented, undermines inferences on catalytic action drawn from experiments performed at atmospheric pressure, where gas-phase oxidation usually plays a dominant role.[2] In this paper we report kinetic and mechanistic results for the low-pressure oxidation of methyl radicals on the active and selective prototype oxide Sm_2O_3,[1,8] obtained in a flow reactor with on-line molecular beam mass spectrometric detection. The gas-phase thermolysis of azomethane is used as a source of methyl radicals,[14] which, at the very low pressures prevalent in these experiments,[15] solely undergo heterogeneous oxidation:

$$CH_3(g) + \gamma_xO(s) \rightarrow CO_x(g) + {}^3/_2H_2O(g) \quad (5)$$

The typical uncertainties associated with active areas of solid catalysts are circumvented by normalizing methyl radical oxidation rates to the rate of reaction 4, measured under identical conditions.[6] In the absence of $O_2(g)$, Sm_2O_3 is almost inert toward methyl radicals, in accord with previous studies by Lunsford et al.[9] We find that in the presence of $O_2(g)$ the

[⊗] Abstract published in *Advance ACS Abstracts,* March 1, 1995.

(1) Lunsford, J. H.; Cisneros, M. D.; Hinson, P. G.; Tong, T.; Zhang, H. *Faraday Discuss. Chem. Soc.* **1989**, *87*, 13 and references therein.

(2) Amenomiya, Y.; Birss, V. I.; Goledzinowski, M.; Galuszka, J.; Sanger, A. R. *Catal. Rev. Sci. Eng.* **1990**, *32*, 163 and references therein. This report explicitly argues that gas-phase oxidation has plagued most studies of methane "catalytic" dimerization.

(3) Mackie, J. C. *Catal. Rev. Sci. Eng.* **1991**, *33*, 169 and references therein.

(4) Feng, Y.; Niiranen, J.; Gutman, D. *J. Phys. Chem.* **1991**, *95*, 6558 and 6564.

(5) Krylov, O. V. *Catal. Today* **1993**, *18*, 209.

(6) (a) Amorebieta, V. T.; Colussi, A. J. *J. Phys. Chem.* **1989**, *93*, 5155. (b) Amorebista, V. T.; Colussi, A. J. *J. Phys. Chem.* **1988**, *92*, 4576.

(7) Rasko, J.; Pereira, P.; Somorjai, G. A.; Heinemann, H. *Catal. Lett.* **1991**, *9*, 395.

(8) Tonkovich, A. L.; Carr, R. W.; Aris, R. *Science* **1993**, *262*, 221.

(9) Tong, Y.; Lunsford, J. H. *J. Am. Chem. Soc.* **1991**, *113*, 4741.

(10) Xu, M.; Rosynek, M. P.; Lunsford, J. H. Reactions of Methyl Radicals with Metal Oxides. Paper presented at the Symposium on Methane and Alkane Conversion Chemistry, Division of Petroleum Chemistry, 207th National Meeting, American Chemical Society, San Diego, CA, March 13−18, 1994.

(11) Wang, D.; Xu, M.; Shi, C.; Lunsford, J. H. *Catal. Lett.* **1993**, *18*, 323.

(12) Grela, M. A.; Amorebieta, V. T.; Colussi, A. J. *J. Phys. Chem.* **1992**, *96*, 7013. We estimate that methyl radicals undergo less than 0.1% oxidation during their residence time ($t_{15} < 10$ ms) in the prereactor at 3 mTorr of O_2, 1300 K, based on our measurements of the rate constant for the following reaction: $CH_3 + O_2 \rightarrow CH_2O + OH$.

(13) Grela, M. A.; Colussi, A. J. Bifurcation Analysis of Methyl Radical Oxidation in Open Systems. The Low Pressure Regime. *Proceedings of the Twenty-Fifth International Symposium on Combustion*, **1994**, in press.

(14) Acs, G.; Peter, A. *Int. J. Chem. Kinet.* **1987**, *19*, 929.

(15) Wagner, A. F.; Wardlaw, D. M. *J. Phys. Chem.* **1988**, *92*, 2462.

0002-7863/95/1517-3856$09.00/0

pseudo-first-order rate constants for methyl radical and methane oxidations on Sm_2O_3, both proportional to $\Gamma([O_2])$,[6b] approach high oxygen pressure limit ratios: $k_5/k_4 \geq 3$, below 1200 K. The thermodynamic parameters characterizing the endothermic O_2 chemisorptions involved in each case are also markedly different. As a consequence, the relative rates of methyl radical oxidation increase at lower temperatures and smaller oxygen pressures.

It seems that this is the first time such information, necessary for a fundamental understanding of the performance of catalyst oxides in the oxidative dimerization of methane, is reported. Thus, based on present results, we can calculate the optimal trade-off between selectivity and methane conversion, i.e. that attained after eliminating all potentially suppressible degradative processes, such as gas-phase oxidations. The heterogeneous oxidation paths of intermediate species do not fall into this category, and represent intrinsic degradative pathways that must be inevitably reckoned with in steady state experiments. However, the fact that the surface centers active in reactions 4 and 5 are kinetically distinguishable reflects underlying structural differences, that eventually may be taken advantage of to selectively oxidize methane on metal oxides.[16]

Experimental Section

The inlet of a heatable flow reactor (fused silica, cylindrical, 5 cm in diameter, 90 cm^3) was connected to a tandem prereactor and its outlet to an analytical mass spectrometer (Extrel). The reactor was operated in the effusive flow regime, characterized by mass-dependent residence times: $t_i = 1/k_{ei} = 7.5(M_i/T)^{1/2}$ s, and gas-wall collision frequencies: $\omega_i = (6.0 \times 10^3)(T/M_i)^{1/2}$ s^{-1} (where the M_i's are molecular masses in daltons).[12,17-19] The independently heated tandem prereactor (1.3 cm^3, $t_i = 0.09(M_i/T)^{1/2}$ s, $\omega_i = (1.4 \times 10^5)(T/M_i)^{1/2}$ s^{-1}), in which methyl radicals are generated by flash pyrolysis of azomethane, was directly attached to the base of the main reactor. Thin beds of catalyst samples (ca. 200 mg) could be rapidly (within $\approx$1 s) inserted or removed along the axis of the main reactor by means of a homemade all-quartz sliding holder. Considering that CH_3 and CH_4 enter the reactor at the same point and that mean free paths at prevalent pressures are of the order of a few centimeters, i.e. that the reactor is well stirred, we assume that all gases flow over the catalyst bed under identical conditions. Hydrocarbon gas-catalyst collision frequencies could be calculated from the following expression: $\omega_{is} = [A_s/(A_s + A_r)](6.0 \times 10^3)(T/M_i)^{1/2}$ s^{-1}, where A_s is the visual area of the catalyst layer and A_r the inner area of reactor walls. We favor the use of visual areas, rather than BET values,[9,10] because under the present conditions mean free paths are far longer than pore sizes, and adsorption of gases other than O_2 can be ignored. Mixtures of azomethane ($0.1 < x_{azo} < 0.8$) and O_2 circulated through the prereactor and reactor sections at flow rates in the range 1−3 nmol/s, corresponding to overall pressures $\leq$3 mTorr. These $[O_2]$'s are considerably smaller than the threshold values required to initiate the branched chain oxidation of methyl radicals in the gas phase.[12] The fast mass spectrometric detection system (EI, 20 eV) for the continuous and simultaneous monitoring of reactants and products, including labile free radicals, has been partially described in detail previously.[17] It consists of a differential pumping chamber, in which a molecular beam is created from the gases exiting the reactor, a collimating orifice, and a second chamber housing a variable speed chopper, an axial electron impact ionizer, and a quadrupole mass analyzer. Signals from the electron multiplier were amplified, fed to a lock-in amplifier, filtered, and acquired by a personal computer for further analysis. Mass scans could be typically programmed to sample each peak for 200 ms or longer, at a frequency of 10 Hz or smaller, depending on the time constant of the lock-in amplifier, and the S/N ratio. Samarium(III) oxide (Aldrich) was conditioned under air at 1073 K for about 8 h before use. This treatment results in partial sintering, which we found necessary to prevent catalyst blowoff upon introduction into the evacuated reactor. Methane and argon (HP, AGA Argentina) were used as received. Azomethane was prepared by oxidation of *N,N'*-dimethylhydrazine (Aldrich) with $Hg^{II}O$,[20] distilled under vacuum, and stored frozen in the dark prior to use.

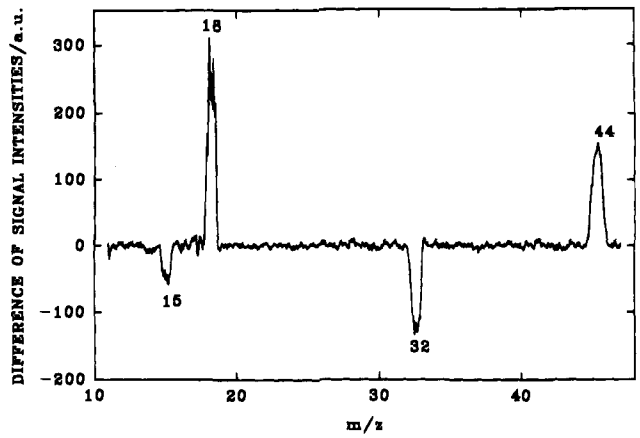

Figure 1. The mass spectrum of the reaction mixture effusing from the reactor in the presence of 70 mg of Sm_2O_3 minus that recorded in its absence. $F(O_2)$ = 0.3 nmol/s; F(azomethane) = 0.08 nmol/s. Reactor temperature: 1090 K. Prereactor temperature: 1300 K.

Results and Discussion

Reaction Products. It is well-established that azomethane decomposes according to reaction 6:

$$CH_3N{=}NCH_3 + M \rightarrow CH_3N{=}N + CH_3 + M \rightarrow 2CH_3 + N_2 + M \quad (6)$$

with a high-pressure first-order rate constant given by[21]

$$\log(k_{6\infty}, s^{-1}) = 15.48 - 11121/T \quad (7)$$

Very recent ab initio calculations show that the intermediate methyldiazenyl radical, $CH_3N{=}N$, with a decomposition barrier of barely 2 kcal/mol, is a fleeting species that splits immediately after being formed.[22] Hence, reaction 6 is a clean source of methyl radicals with a fixed stoichiometry $|\Delta(CH_3)/\Delta(\text{azomethane})| = 2$. Under the present conditions, reaction 6 takes place in its pressure fall-off region. The collision frequency ω_i prevalent in the prereactor leads, with a gas-wall collision efficiency of $\beta_w \approx 0.5$,[12] to a fall-off factor of about 0.002, and to a rate constant of $k_6 \approx 2 \times 10^4$ s^{-1} at 1300 K. Thus, we estimate that less that 1% azomethane survives passage through the prereactor at this temperature. The absence of ion signals at $m/z = 58$ ($CH_3N_2CH_3^+$) and 43 ($CH_3N_2^+$), in the mass spectrum of the products effusing from the empty reactor, confirmed these expectations.

In Figure 1 we show the difference between the mass spectrum obtained for a 1:3 azomethane−oxygen mixture in the presence of 70 mg of Sm_2O_3 at 1090 K and that recorded in its absence. The total pressure in the reactor is about 0.4 mTorr, corresponding to a mean free path of about 15 cm and to a gas−gas collision frequency of about 570 s^{-1}. Clearly, O_2 ($m/z = 32$) and CH_3 ($m/z = 15$) are consumed in the presence

(16) Amorebieta, V. T.; Colussi, A. J. Submitted for publication.
(17) Amorebieta, V. T.; Colussi, A. J. *J. Phys. Chem.* **1982**, *86*, 2760.
(18) Golden, D. M.; Spokes, G. N.; Benson, S. W. *Angew. Chem., Int. Ed. Engl.* **1973**, *12*, 534.
(19) Tabor, K.; Gutzwiller, L.; Rossi, M. J. *J. Phys. Chem.* **1994**, *98*, 6172.
(20) Renaud, R.; Leitch, L. C. *Can. J. Chem.* **1954**, *32*, 545.
(21) NIST Chemical Kinetics Database, Version 2.01, F. Westley, J. T. Herron, R. J. Cvetanovic, R. F. Hampton, and W. G. Mallard; National Institute of Standards and Technology: Gaithersburg, MD, 1990.
(22) Hu, C.-H.; Schaefer, H. F. *J. Chem. Phys.* **1994**, *101*, 1289.

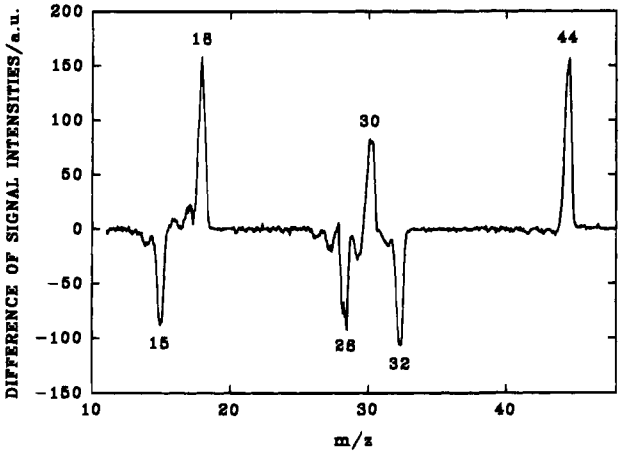

Figure 2. The mass spectrum of the reaction mixture effusing from the reactor in the presence of 70 mg of Sm_2O_3 minus that recorded in its absence. $F(O_2)$ = 0.3 nmol/s; F(azomethane) = 0.21 nmol/s. Reactor temperature: 1090 K. Prereactor temperature: 400 K.

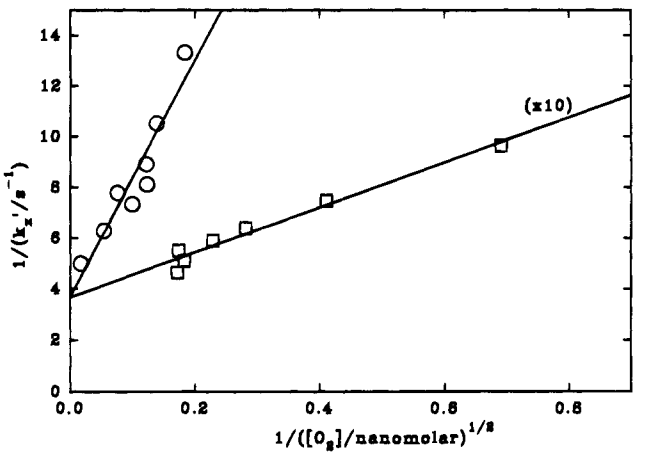

Figure 3. Reciprocals of pseudo-first-order rate constants for the oxidation of methyl radicals (squares) and methane (circles) on 240 mg of Sm_2O_3 vs the reciprocal of the square root of steady state O_2 concentrations, at 1010 K.

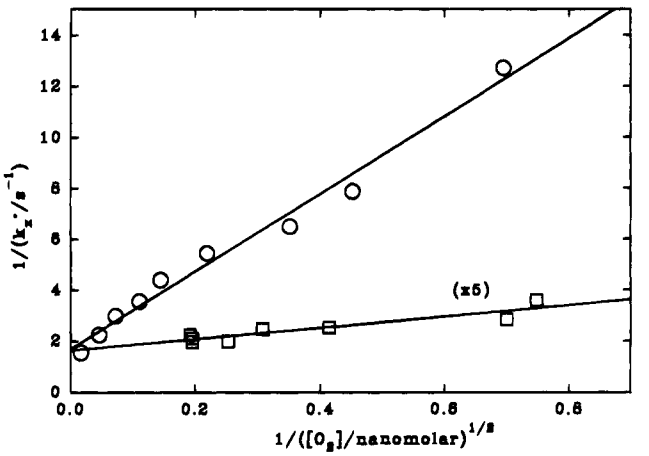

Figure 4. Same as in Figure 3, but at 1100 K.

of catalyst, producing water (m/z = 18) and carbon dioxide (m/z = 44). Based on an experimental calibration of the relative sensitivities of the m/z = 44 and 15 signals at 20 eV, $I_{15}/(k_{e,15}[CH_3]) = 0.19I_{44}/(k_{e,44}[CO_2])$, we find that CO_2 accounts for (100 ± 20)% of methyl losses, under the conditions of Figure 1. The CO_2 yield drops to about 60%, the remainder being CO, for a 1:4.58 azomethane–oxygen mixture, at a total pressure of 0.7 mTorr. However, CO and CO_2 both must be considered primary gaseous products, and their branching determined prior desorption, because secondary CO(g) oxidation on Sm_2O_3 is too slow to lead to a 100% CO_2 yield in this setup.[16] These carbon balances actually correspond to the steady state regime that attains after the solid has equilibrated with the overhead gas, and they are therefore independent of any CO_2 adsorption on Sm(III) oxide.

In some experiments, not shown, carried out at larger azomethane flow rates, small negative signals at m/z = 29 and 30, corresponding to loss of C_2H_6, were also apparent. They arise from the heterogeneous oxidation of minor amounts of ethane, which are formed in the prereactor under such conditions. Since the mass spectrum of ethane lacks a m/z = 15 fragment at 20 eV, and no recombination of methyl radicals ever takes place inside the main reactor, the presence of ethane traces can be ignored in the evaluation of k_5 (see below). The prolonged exposure of surfaces to methyl radicals in the absence of oxygen results in the formation of carbon deposits.[12] However, minute oxygen flow rates are already sufficient to prevent the growth of such deposits that apparently catalyze the breakdown of methyl radicals. The onset of the homogeneous oxidation of CH_3 occurs at much larger O_2 concentrations, as studied previously.[12]

We found that if the prereactor is cooled down to about 400 K, the resulting mass spectra change rather dramatically, see Figure 2. In this case N_2 (m/z = 28) is depleted along with CH_3 and O_2, and besides H_2O and CO_2, a new species of molecular mass 30 is formed. After eliminating C_2H_6 and H_2-CO as possible identities for the latter species, based on the fact that their mass spectra possess intense m/z = 29 fragments (at variance with the spectrum of Figure 2), and bearing in mind that N_2 is also consumed, we are led to conclude, somewhat to our amazement, that unreacted azomethane is partially oxidized to NO (n/z = 30) on Sm_2O_3. In other words, the thermalization of azomethane molecules competes with their heterogeneous oxidation during gas–solid collisions, revealing an extraordinarily large efficiency ($\gamma \approx 0.3$) for the latter process. Further details will be published elsewhere.[16] To avoid these complications, the following analysis deals throughout with experiments performed with the prereactor maintained at 1300 K.

Kinetic and Thermodynamic Results

Pseudo-first-order rate constants for the heterogeneous oxidation of methyl radicals, k_5', or methane, k_4', were calculated from the expression[12]

$$k_x' = k_{e,x} f/(1 - f) \qquad (8)$$

where the rate constant for the escape of methyl radicals is given by $k_{e,15} = (3.44 \times 10^{-2})T^{1/2}$ s^{-1}, $k_{e,16} = 0.97k_{e,15}$, and $f = (I_{woc} - I_{wc})/I_{woc}$ is the fraction of methyl radicals (or methane) oxidized on the catalyst; I_{wc} and I_{woc} are the steady state intensities of the m/z = 15 (16) signal, with and without catalyst, respectively, at constant T. We verified that k_x' values calculated from eq 8 are actually independent of methyl radical (or methane) flow rates in the range 0.05–0.20 nmol/s, confirming the assumed first-order kinetics.

The derived k_x' values depend on O_2 flow rates in a nonlinear manner. In Figures 3–5 we present plots of $(1/k_x')$ values measured on the same oxide sample vs $(1/[O_2]_{ss}^{1/2})$ at 1010, 1100, and 1200 K, respectively. As shown in previous studies of methane oxidation on oxides,[4,6] the linearity of such plots implies a rate law: $-d[X]/dt = k_x[X]K_x^{1/2}[O_2]^{1/2}/(1 + K_x^{1/2}[O_2]^{1/2})$. This type of kinetics can be easily rationalized by assuming that the reactive surface oxygen species O(s) that appear in rate

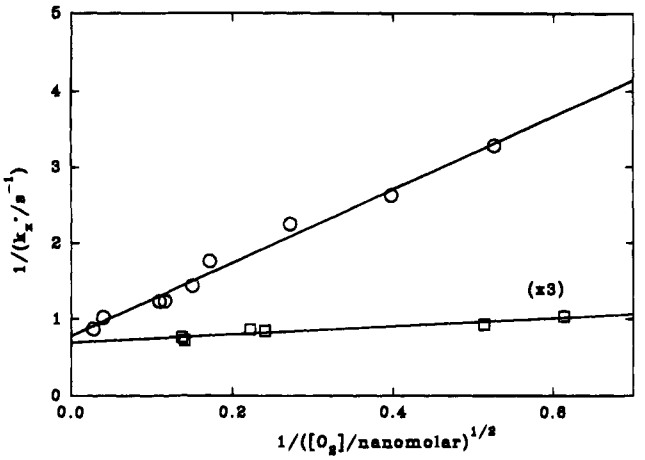

Figure 5. Same as in Figure 4, but at 1200 K.

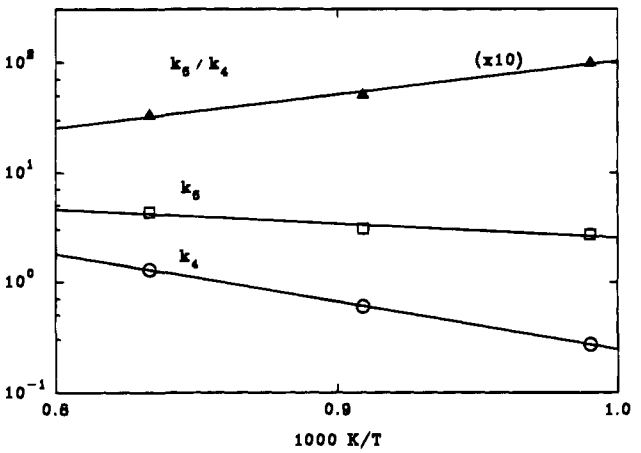

Figure 6. Arrhenius plots for the individual first-order rate constants of steps 4 and 5, and for their ratio.

determining steps 4 and 5 are in dissociative equilibrium with O_2(g), or, alternatively, with a O_2(s) species whose concentration is proportional to O_2(g):[4,6]

$$O_2(g) \rightarrow O_2(s) \quad (9)$$

$$O_2(s) \rightarrow O_2(g) \quad (-9)$$

$$O_2(s) \leftrightarrow 2O(s) \quad (10)$$

According to this interpretation, the reciprocals of the intercepts in Figures 3–5 yield the desired k_4 and k_5 rate constants; from the slopes, one can immediately derive the equilibrium constants for O_2 chemisorption: $K_x = K_9K_{10}$. Arrhenius plots for the different kinetic and thermodynamic constants are shown in Figures 6 and 7, and the corresponding parameters are collected in Table 1. The activation energies of the elementary rate determining steps 4 and 5 (E_4 = 19.9 kcal/mol and E_5 = 6.2 kcal/mol) should not be confused with overall activation energies calculated from rates measured at *constant* $[O_2]$.

The widely different van't Hoff parameters for K_4 and K_5 in Table 1 indicate that *the O(s) species responsible for methyl oxidation is not identical with that active in step 4*. This is a particularly important finding which, given the dissimilar nature of these reactions, could perhaps have been anticipated. Observe that step 4 involves an H-atom transfer to the oxide, while step 5 formally amounts to an O-atom displacement in the opposite direction to trap the incoming CH_3 as a CH_3O(s) fragment. Remarkably, but obviously in line with the observed endothermicities, the entropy changes associated with O_2 chemisorptions are very large: ΔS_4° = 39 cal/(K mol), ΔS_5° = 56 cal/(K mol) (standard state: 1 atm ideal gas, $\langle T \rangle$ = 1100 K). Considering that ΔS = 30 eu at 1100 K for the gas-phase dissociation O_2(g) = 2O(g), we conclude that the endothermic O_2-chemisorption processes preceding reactions 4 and 5 on Sm_2O_3 and other oxides[4,6] do not take place on a rigid lattice, but must be associated with cooperative disordering of the solid. Such transformation, as yet unidentified, actually provides the entropic driving force for these uphill processes to occur, and may represent the ultimate cause of catalytic action.[23,24]

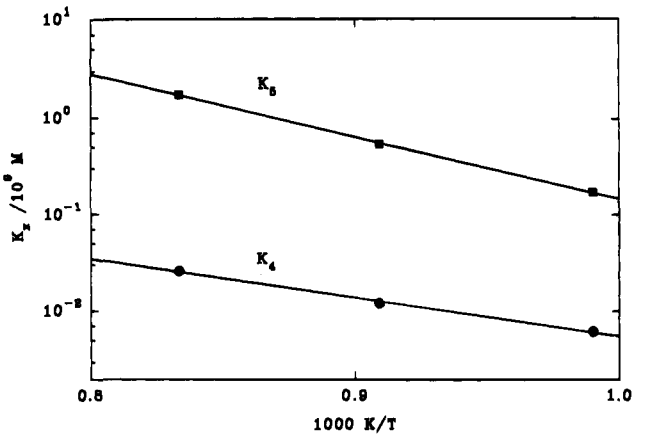

Figure 7. van't Hoff plots for the overall equilibrium constants K_4 and K_5 of O_2 chemisorption leading to the active species in reactions 4 and 5, respectively. See text.

Table 1. Kinetic and Thermodynamic Data

	1010 K	1100 K	1200 K
k_4 (s^{-1})[a]	0.27 ± 0.05	0.60 ± 0.09	1.29 ± 0.10
	$\log(k_4/s^{-1})^b = (3.73 \pm 0.45) - (4350 \pm 50)/T$		
k_5 (s^{-1})	2.73 ± 0.19	3.06 ± 0.31	4.33 ± 0.20
	$\log(k_5/s^{-1}) = (1.76 \pm 0.36) - (1350 \pm 330)/T$		
	$\log(k_5/k_4) = -(2.18 \pm 0.35) + (3210 \pm 301)/T$		
$K_4/10^9$ (M)	$(6.2 \pm 4.0) \times 10^{-3}$	$(1.2 \pm 0.5) \times 10^{-2}$	$(2.6 \pm 0.6) \times 10^{-2}$
	$\log(K_4/10^9\ M) = (1.89 \pm 0.25) - (4170 \pm 260)/T$		
$K_5/10^9$ (M)	0.17 ± 0.05	0.55 ± 0.29	1.75 ± 0.75
	$\log(K_5/10^9\ M) = (5.65 \pm 0.11) - (6480 \pm 130)/T$		

[a] Absolute values of rate constants measured on 240 mg of Sm_2O_3; see text. Only the ratio (k_5/k_4) is independent of catalyst mass or active area. [b] Arrhenius parameters calculated by linear regression with weights proportional to (1/standard error) of the rate or equilibrium constants at each temperature.

We wish to point out that methyl radical concentrations were independent of moderate O_2 flow rate variations *in the absence of catalyst* and that methyl radicals still undergo oxidation on the catalyst after O_2(g) has been removed from the reactor (see below). Both observations exclude gas-phase reactions under the present conditions, and confirm the purely heterogeneous nature of the processes we are describing.

In principle, measured rates of methyl radical heterogeneous oxidation should be scaled to unit area of catalyst. Such scaling is always uncertain because active areas are, in general, reaction sensitive, and therefore not transferable. The use of BET areas

(23) (a) Haber, J. in *Catalysis of Organic Reactions*; Kosak, J. R., Johnson, T. A., Eds.; Marcel Dekker: New York, 1994; p 151. (b) Bielanski, A.; Haber, J. *Oxygen in Catalysis*; Marcel Dekker: New York, 1991; Chapter 4 and references therein. Rao, C. N. R.; Gopalakrishnan, J. *New Directions in Solid State Chemistry*; Cambridge University Press: Cambridge, 1986; Chapter 5.

(24) Kosuge, K. *Chemistry of Non-stoichiometric Compounds*; Oxford University Press: Tokyo, 1994; Chapter 1.

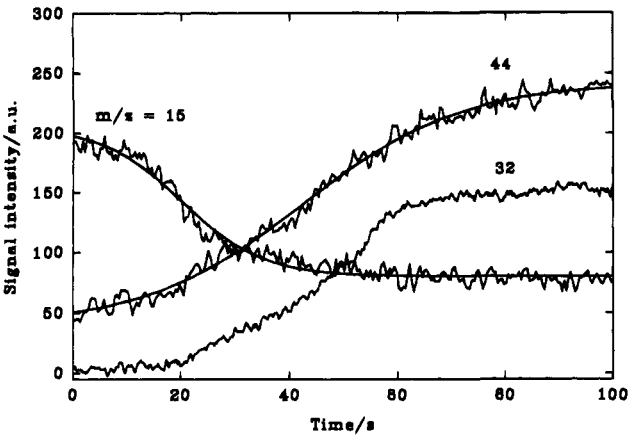

Figure 8. Transient signals of methyl radicals (m/z = 15), oxygen (m/z = 32), and carbon dioxide (m/z = 44), following step function admission of O_2(g) at time zero, over a catalyst bed that had been maintained under steady methyl flow during the previous 5 min. $F(O_2)$ = 2.0 nmol/s, F(azomethane) = 0.4 nmol/s. Reactor temperature: 1100 K. Prereactor temperature: 1300 K. The solid curves are nonlinear least-squares fits (calculated with SigmaPlot5.0WIN) of logistic functions: $f(t) = \{p_1/[1 + \exp(p_2(t - p_3))]\} + p_4$; $p_3(CH_3)$ = 20.2 s; $p_3(CO_2)$ = 42.5 s.

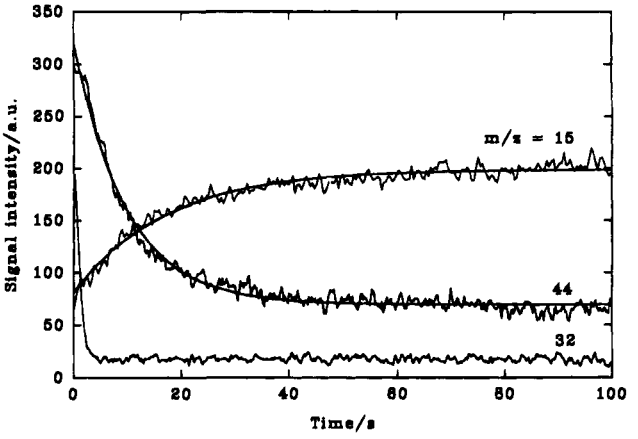

Figure 9. Transient signals for methyl radicals (m/z = 15), oxygen (m/z = 32), and carbon dioxide (m/z = 44), following the interruption of the O_2(g) flow after the steady state regime was reached in the experiment of Figure 8. Notice that the initial m/z = 32 and 44 signal intensities are larger than the those at 100 s in Figure 8, revealing the slow approach of both species to steady state. The solid curves are nonlinear least-squares fits of exponential functions. The characteristic time constants are 17.2 s for CH_3 and 9.6 s for CO_2.

is also questionable at low pressures because, unless they become adsorbed, reactant molecules can hardly explore catalyst pores having dimensions much smaller than mean free paths. Since our ultimate goal is to use the present data in the kinetic analysis of the oxidative coupling of methane, we avoided this limitation by normalizing k_5 values to the rate constants for methane oxidation k_4, *measured at the same temperature, and catalyst mass*, either simultaneously or in back-to-back experiments (see Figure 6). The basic assumption underlying this scaling procedure is that the steady state distribution of surface sites active in steps 4 and 5 is independent of catalyst history or morphology. This contention is certainly less objectionable than invoking active areas determined by other methods or under different experimental conditions. More importantly, the relative rates calculated from eq 1, and shown in Figure 6, are directly relevant to the issue at hand. Clearly, present results are not comparable to the rates of methyl radical oxidation on metal oxides measured in the absence of O_2(g).[9,10]

Transient Experiments

Transient experiments, performed by applying step-function O_2(g) flows, provided further clues regarding the mechanism of methyl radical oxidation on samarium(III) oxide. In Figure 8 we show the transient m/z = 15, 32, and 44 signals, simultaneously acquired after the admission of O_2(g) to the reactor containing a catalyst sample that had been subjected to a steady flow of CH_3(g) for 5 min, at 1100 K. Figure 9 shows the signals following interruption of the O_2 flow, after steady state was reached in the experiment of Figure 8.

Several features in Figure 8 deserve attention. The slow sigmoid, rather than the fast exponential, approach of O_2(g) to steady state is due to rapid oxygen uptake by the solid, during the initial stage, followed by a coverage-dependent adsorption rate.[25,26] As a reference, the empty reactor could be filled to $[O_2]_{ss}/2$ within 0.88 s. On the other hand, the evolution of the

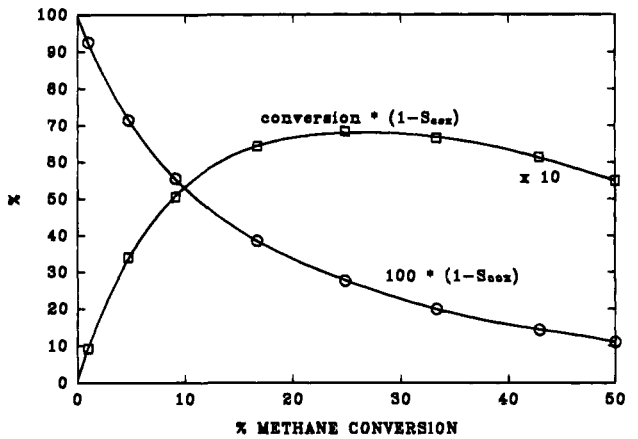

Figure 10. Results of the integration of a mechanism comprising reactions 4 and 5 (with β = 1, $k_5' = 8k_4'$) and the inflow of CH_4 and escape of all species, which describes methane oxidation over Sm_2O_3 in *our* low-pressure reactor at ca. 1100 K. Open circles and curve: the percentage yield of non-CO_x species ($S_{CO_x} = \Delta(CO_x)/\Delta(CH_4)$, is the selectivity of CO_x production); Open squares and curve: 10[(percent methane conversion)(1 − S_{CO_x})].

m/z = 15 signal, which displays a slow initial rate followed by sudden acceleration to a maximum at 20.2 s, leads the $[O_2]$ profile by more than 25 s. This is indicative of low reactivity toward CH_3 by the early-filled active oxygen sites, and it is consistent with a less-than-linear dependence of the concentration of the effectively reactive sites on $[O_2(g)]$. Finally, the inflexion time for the CO_2 curve, corrected for the relative residence times of CH_3 and CO_2 ($\tau_{i,corr}(CO_2) = (15/44)^{1/2}\tau_i(CO_2)$ = 42.5 × 0.58 = 24.7 s) is only a few seconds longer than $\tau_i(CH_3)$, implying that the surface oxidation processes ensuing methyl capture are fast, and that CO_2 is weakly or slowly adsorbed at these temperatures and pressures.[16]

Figure 9 also contains valuable information. The fact that $[O_2(g)]$ falls off as rapidly as if the reactor were empty, although the catalyst is still active, reveals slow O_2 desorption.[25] The ongoing methyl radical oxidation after O_2(g) drops to zero is direct evidence of exclusive heterogeneous oxidation. Moreover, the relatively slow recovery of $[CH_3]_{ss}$ proves that the dissociative O_2(s) ↔ 2O(s) equilibrium, implicated by the rate laws for reactions 4 and 5, only involves surface species, rather

(25) Amorebieta, V. T.; Colussi, A. J. Reactive vs. Adsorbed Oxygen in the Heterogeneous Oxidation of Methane over Li/MgO; Paper presented at the Symposium on Methane and Alkane Conversion Chemistry, Division of Petroleum Chemistry, 207th National Meeting, American Chemical Society, San Diego, CA, March 13−18, 1994.

(26) Adamson, A. W. *Physical Chemistry of Surfaces*, 5th ed.; Wiley: New York, 1990; p 651 and Chapter XVII.

than $O_2(g)$ as previously assumed,[6] and confirms the slowness of step (−9).[27] Actually, the formation of O(s) by direct impact of $O_2(g)$ would be immeasurably slow. We estimate an *A*-factor value of $A_9 \approx 1.5 \times 10^2$ s^{-1} at 1100 K, by assuming a unitary sticking coefficient.[28] Hence, the creation of the endothermic O(s) (ΔH = 27.4 kcal/mol, see Table 1) species responsible for the oxidation of CH_3 would take place with a first-order rate constant of about 1.6×10^{-4} s^{-1}, i.e. with a time constant of about 1.8 h! It is more realistic to assume that $O_2(g)$ is first attached to the surface, step 9, before undergoing dissociation in a process, step 10, having a much larger *A* factor.[28] A simple calculation also reveals that the CO_2 produced during the concomitant oxidation of CH_3 cannot account for the relatively slow decay of the m/z = 44 signal; substantial amounts of CO_2 must be released from the solid in this stage. However, it is not clear yet whether the excess CO_2 comes from a pool slowly created during steady state conditions or, less likely, from the slow oxidation of a bound intermediate precursor at $[O_2(g)] = 0$.[27] Finally, it is apparent that even 100 s after shutting off $O_2(g)$, some CO_2 is still being formed, but at a rate about 6 times slower than under $[O_2(g)]_{ss}$. Measurements at a much longer time scale show further reduction of catalyst activity, in line with previous observations on lattice oxygen depletion.[25]

Implications for the Oxidative Coupling of Methane

There has been much debate regarding the basal or minimal yield of carbon oxides that could be attained in the oxidative dimerization of methane on metal oxides.[29-31] This issue is inextricably linked to the nature of possible CO_x sources in these systems. In principle, if $\beta = 1$ (eq 4), one could completely shun CO_x species by preventing secondary oxidation of methyl radicals and later generation species. However, present results show that the heterogeneous oxidation of methyl radicals represents an irreducible process that cannot be entirely defeated. To illustrate the point, in Figure 10 we present the yields of non-CO_x products in the partial oxidation of a methane/oxygen mixture fed to our catalytic reactor at a steady CH_4 flow rate of 2 nmol/s. These values were calculated by means of a core mechanism comprising reactions 4 and 5, with $\beta = 1$, $k_5' = 8k_4'$, i.e. at sufficiently large $[O_2]$ to approach the limiting ratio given by eq 1 at ca. 1010 K, or at any higher temperature, but at lower oxygen pressures. At typical collision frequencies the association of methyl radicals is a very slow process,[15] and the local gas-phase formation of C_2 species can be ignored. We find a modest maximum 7% yield of non-CO_x products at about 25% methane conversion. The inverse temperature dependence of the (k_5/k_4) ratio lets us predict smaller methane conversions *and* poorer selectivities at lower temperatures and pressures.[2] Extensions of this calculation to pressures high enough that methyl radical association should be taken into account will require information on the rates and products of the heterogeneous oxidations of higher generation species, such as ethane and ethylene. This approach to the estimation of optimal C_2 yields, and indirectly to process design, is based on the concept that it is possible to operationally disengage gas-phase combustion processes from heterogeneous oxidations by maintaining the reacting mixture in the preignition regime.[8,13] Notice that the above analysis does not apply to nonstationary conditions, which pose different challenges, but open new dimensions, to CO_x control.[32] We are actively exploring these issues.[16]

Conclusions

We report new, direct measurements of the relative rates of methyl radical and methane oxidations on Sm_2O_3 in the presence of gaseous oxygen, under steady state conditions above 1000 K. The products of methyl radical oxidation have been identified, and the carbon balance quantified. Transient phenomena induced by the injection or removal of $O_2(g)$ have been qualitatively analyzed in relation to the mechanism of heterogeneous methyl radical oxidation. Two important facts emerge: (1) methyl radicals are oxidized faster than methane, and (2) each species reacts on quantitatively different chemisorbed O(s) active sites. Present kinetic results have been used to evaluate the minimum yield of CO_x species that could be obtained in the steady state oxidation of methane at low pressures and to propose a rational approach to the analysis of methane oxidative dimerization based on the decoupling of homogeneous and heterogeneous processes.

Acknowledgment. This project was financially supported by CONICET/Argentina, under Grant PID/1131-91.

JA943481T

(27) Buyevskaya, O. V.; Rothaemel, M.; Zanthoff, H. W.; Baerns, M. *J. Catal.* **1994**, *150*, 71. This paper, which appeared after submission of our manuscript, reports $^{18}O_2$ exchange experiments showing that "...oxygen activation on the surface is faster than activation of methane...", and that "...surface reaction of methane with oxygen intermediates formed from gas-phase O_2 is faster than the desorption of any diatomic oxygen species...", confirming our findings.

(28) Baetzold, R. C.; Somorjai, G. A. *J. Catal.* **1976**, *45*, 94.

(29) Labinger, J. A.; Ott, K. C. *J. Phys. Chem.* **1987**, *91*, 2682.

(30) Labinger, J. A. *Catal. Lett.* **1987**, *1*, 371.

(31) Shi, C.; Rosynek, M. P.; Lunsford, J. H. *J. Phys. Chem.* **1994**, *98*, 8371.

(32) Villermaux, J. *Chem. Eng. Sci.* **1993**, *48*, 2525.